SCIENTIFIC REPORTS

OPEN

SUBJECT AREAS:
CARBON NANOTUBES AND FULLERENES
MECHANICAL ENGINEERING
ELECTRICAL AND ELECTRONIC ENGINEERING

Received
9 June 2014

Accepted
29 July 2014

Published
18 August 2014

Correspondence and requests for materials should be addressed to Y.H.K. (yongkim@snu.ac.kr)

* These authors contributed equally to this work.

Nanotube Aerogel Sheet Flutter for Actuation, Power Generation, and Infrasound Detection

Tae June Kang[1]*, Taewoo Kim[2]*, Eui Yun Jang[2], Hyeongwook Im[2], Xavier Lepro-Chavez[3], Raquel Ovalle-Robles[3], Jiyoung Oh[3], Mikhail E. Kozlov[3], Ray H. Baughman[3], Hong H. Lee[4] & Yong Hyup Kim[2]

[1]Department of NanoMechatronics Engineering and BK21 Plus Nano Convergence Technology Division, College of Nanoscience and Nanotechnology, Pusan National University, Busan 609-735, South Korea, [2]School of Mechanical and Aerospace Engineering, Seoul National University, Seoul 151-744, South Korea, [3]The Alan G. MacDiarmid NanoTech Institute, The University of Texas at Dallas, Richardson, TX 75083, USA, [4]School of Chemical and Biological Engineering, Seoul National University, Seoul 151-744, South Korea.

Electromagnetic induction (EMI) is a mechanism of classical physics that can be utilized to convert mechanical energy to electrical energy or electrical to mechanical energy. This mechanism has not been exploited fully because of lack of a material with a sufficiently low force constant. We here show that carbon nanotube (CNT) aerogel sheets can exploit EMI to provide mechanical actuation at very low applied voltages, to harvest mechanical energy from small air pressure fluctuations, and to detect infrasound at inaudible frequencies below 20 Hz. Using conformal deposition of 100 nm thick aluminum coatings on the nanotubes in the sheets, mechanical actuation can be obtained by applying millivolts, as compared with the thousand volts needed to achieve giant-stroke electrostatic actuation of carbon nanotube aerogel sheets. Device simplicity and performance suggest possible applications as an energy harvester of low energy air fluctuations and as a sensor for infrasound frequencies.

Electromagnetic induction is the production of a potential difference (voltage) across a conductor when it is exposed to a varying magnetic field[1]. A potential difference is also generated across the conductor when it is made to vibrate or deflect in the presence of a constant magnetic field. On the other hand, the conductor deflects or vibrates in a constant magnetic field when a constant or oscillating potential difference is applied across the conductor. Electromagnetic induction using carbon nanotubes (CNTs) has been exploited for determination of Young's modulus[2], nanoscale traveling-wave-tube amplifiers[3], and nanomechanical resonators[4].

Our motivation for coupling CNT aerogel sheet using electromagnetic induction lies in the special features of CNT sheets. While the carbon nanotube aerogel sheets have a density (~1.5 mg/cm^3) that is close to that of air[5], their gravimetric strength (~130 MPa/(g/cm^3)) is comparable to that of the Mylar and Kapton films used for ultralight air vehicles (~160 MPa/(g/cm^3)) and that of ultra-high-strength steel sheets (~125 MPa/(g/cm^3))[6]. Additionally, the sheet density is typically only about 2 μg/cm^3, which makes them deformable by small stresses, and they are electronically conducting. The CNT sheets are easily elastically bent by electromagnetically induced forces or fluctuations in air pressure, since the measured Young's modulus of the investigated CNT aerogel sheet is only about 11.5 MPa (Table S1), compared with the 2.8 GPa for Mylar film, and the ratio of sheet length (5.5 to 12 cm) to sheet thickness (~20 μm) is giant.

Results

Nanotube Aerogel Sheet Flutter for Actuation. The electromagnetic induction (EMI) device we fabricated and used for various purposes has a simple structure: A CNT sheet is suspended between a pair of rigid copper wire electrodes that is placed in a homogeneous magnetic field, as schematically illustrated in Figure 1a. For the fabrication of this CNT-sheet electromagnetic induction device, CNT sheets were drawn from a sidewall of a carbon multi-wall nanotube (MWNT) forest by a dry-state draw process[5,7], which typically yields an areal density in the sheet plane of ~2 μg/cm^2 and a thickness of ~20 μm. The as-drawn CNT sheet was attached to the

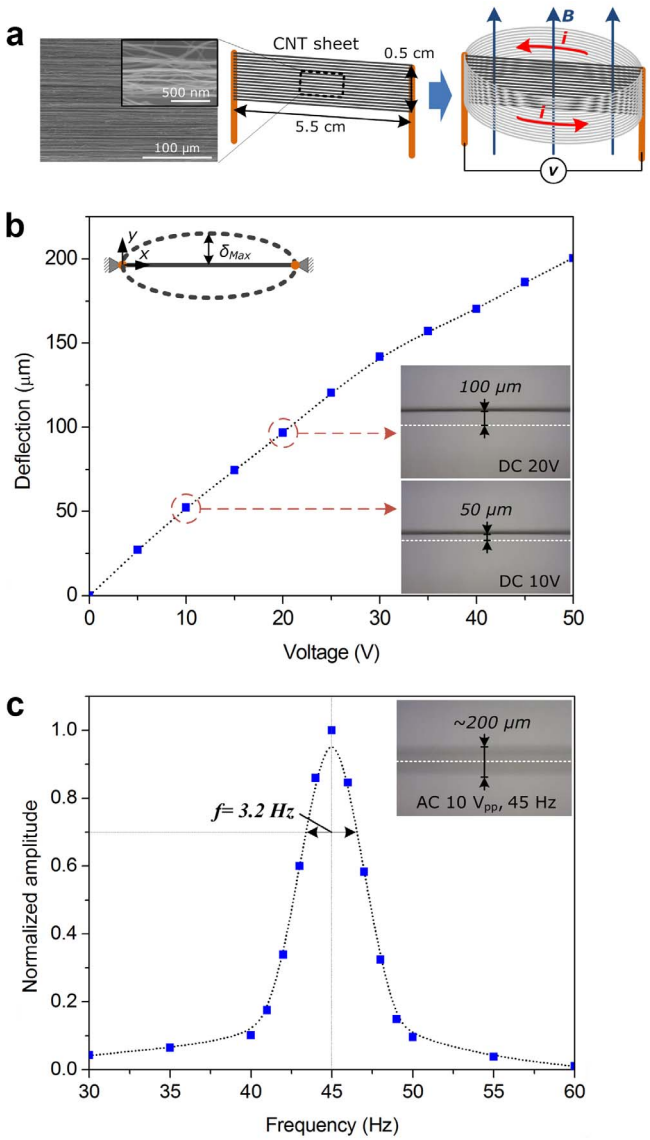

Figure 1 | Electromagnetic actuation of a CNT aerogel sheet. (a) A CNT aerogel sheet (suspended between a pair of copper wire electrodes) is placed in a homogeneous magnetic field. SEM images of the CNT sheet are shown on the left (along with a schematic illustration of the suspended sheet). A Lorentz force, which is produced when a voltage is applied between the electrodes (along the CNT alignment direction of the CNT sheet) causes the sheet to flap in opposite directions depending upon the direction of the resulting current, relative to the direction of the magnet field. (b) The static deflection (δ_{max}) of the sheet is plotted as a function of DC voltage. Optical images of the transversely deflected nanotube sheet are shown in the inset. (c) Normalized oscillation amplitude is plotted as a function of the driving frequency. The optical image of vibration mode at the first resonance frequency is shown in the figure inset.

electrodes with a thin layer of silver paste coated onto the electrodes, which was subsequently dried in air. A homogeneous magnetic flux density (B) of 0.3 Tesla was applied across the CNT sheet using a permanent magnet.

This simple device was utilized to characterize actuation for CNT sheets. Magnetic force (Lorentz force), F_L, is produced when a voltage (V) is applied across the CNT sheet in the presence of a magnet, which causes the sheet to flap, as illustrated in the third frame of Figure 1a. The Lorentz force is given by $B{\cdot}(V/R){\cdot}L$, where R and L represent the resistance and length of the sheet, respectively. Static deflection occurs when a direct current (DC) voltage is applied, as shown in Figure 1b, where static deflection is plotted as a function of applied voltage. The deflection shows a quasi-linear relationship with applied voltage. Since the individual string of nanotubes composing the sheet has a very large aspect ratio (the sheet length/nanotube diameter), the bending stiffness is negligible compared to the axial stiffness. Therefore, the nanotubes behave like elastic strings when they are subjected to transversely applied force (*i.e.* the Lorentz force). In this case the static deflection of the nanotube sheet is linearly proportional to the force, which in turn has a linear relationship with the applied voltage ($F_L{\sim}V$). Optical images of the transversely deflected nanotube sheet are shown in the inset of Figure 1b. Static transverse deflections (δ_{max}) of the nanotube sheet were found to be ~50 and 100 μm at the midpoint of the sheet when the applied DC voltages were 10 and 20 V, respectively. To show the deflection clearly, the initial position with no voltage applied is marked with a dotted line in the image. The deflection increases with increasing voltage but over 30 V, it deviates from the linear relationship due to nonlinear stiffening effect of the nanotubes with clamped boundary conditions at both ends[8].

The CNT sheet vibrates when an alternating current (AC) voltage is applied, instead of a DC voltage. Resonant vibration occurs when the driving frequency matches the natural frequency of the CNT sheet. Figure 1c shows, for actuation in air, the normalized oscillation amplitude as a function of the driving frequency that resulted when an AC peak-to-peak voltage (V_{pp}) of 10 V was applied to the sheet. The first resonance of the sheet was observed at 45 Hz. An optical image of the vibration mode at this first resonance frequency is shown in the Figure 1c inset (see also movie clip 1). A quality (Q) factor of ~14 was obtained by dividing the resonance frequency by the width of the resonance peak at $\sqrt{2}/2$ of the maximum amplitude[9]. The resonance frequency and Q factor are markedly lower than those (1089 Hz and 455, respectively) measured in vacuum for a nanotube sheet having similar dimensions[7]. The differences indicate that viscous damping of air changes the actuation characteristics of the sheet, due to its extremely low inertia and high specific surface area in a low Reynolds number regime ($Re \sim 2 \times 10^{-5}$, Supplementary Information 1)[10–12].

The CNT-sheet EMI device, which is called a CNT sheet flutter, utilizes the Lorentz force that is produced by electrical current in a magnetic field. Therefore, actuation modes of CNT sheet can easily be modulated by changing sheet orientations with respect to an external magnetic field. The sheet can be made to actuate in either in-plane or out-of-plane directions (Supplementary Information 2, and movie clips 2 and 3), and can even be made to feather, by allowing a tension gradient along a sheet width direction (movie clips 4 and 5).

It is highly desirable for the actuation voltage to be as low as possible[13,14]. The above expression for Lorentz force shows that the actuation voltage can be reduced by decreasing the resistance of the CNT sheet. One way of decreasing this resistance is to conformably coat the CNT fibres in the sheet with a metal. Figure 2a shows the dependence of sheet resistance on the thickness of aluminum coated onto the nanotube sheet (see Method and Supplementary Information 3 for details).

As apparent from Figure 2b and its inset, the electrical power needed to achieve the same deflection of the CNT sheet is lowered by three orders of magnitude by coating the sheet with a 100 nm thick layer of aluminum. This coating increased sheet density from 1.5 to 7.2 mg/cm^3, increased areal density from 2 to 14 μg/cm^2, increased elastic modulus from 11.5 to 53 MPa, but little affected sheet strength (changing from ~206 to ~217 kPa), and decreased sheet resistance from ~880 to 5.5 ohm/sq, as shown in Table S1. Only millivolts of voltage are required to actuate CNT sheet when electromagnetic induction is used. In contrast, a kilovolt size voltage was needed to provide giant-stroke non-resonant actuation of the

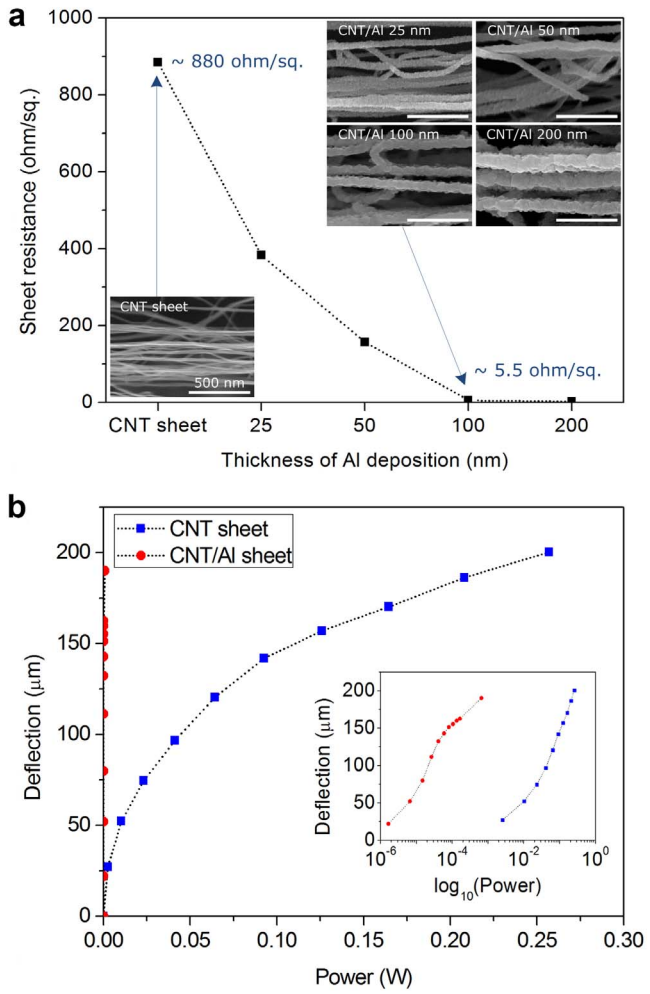

Figure 2 | Experimental results for CNT sheets in which an aluminium layer has been deposited on the surface of individual CNT and CNT bundles. (a) The sheet resistance decreases markedly with increasing thickness of the metal layer deposited on the carbon nanotube aerogel sheet - the original sheet resistance of 880 ohm/sq reduces to 5.5 and 2.2 ohm/sq as the metal layer thickness increases from 100 nm to 200 nm, respectively. The surfaces of individual MWNTs and MWNT bundles in the sheet are uniformly coated with Al layers, as shown in the figure insets. (b) Sheet deflection as a function of applied electrical power. The electrical power needed to achieve the same deflection of the CNT sheet is lowered by three orders of magnitude by coating the sheet with 100 nm thick layer of Al.

sheet by using electrostatic repulsive force[7]. While the extremely low density of these sheets means that they can accomplish little mechanical work during actuation cycles, very low power and voltage consumption realized by electromagnetic induction should be helpful for the development of electrically powered actuations based on CNT sheet.

Power generation. The deflection and vibration of CNT sheet due to the applied voltage and magnetic field immediately suggests the other side of electromagnetic induction, namely generation of electricity from movement of a CNT sheet. With the power requirements for microelectronics ever decreasing, use of ambient energy sources is becoming feasible for either replacing or augmenting battery usage[15,16]. One of the most widely available forms of ambient energy is air movement, such as acoustic noise[17–21] and gentle breezes[22–25], which exist virtually everywhere and are essentially inexhaustible.

Since the carbon nanotube sheet is an aerosol having about the density of air, as well as very low areal density, even minor disturbances in the surrounding air causes the CNT sheet to deflect. This movement of the CNT sheet in the magnetic field enables capture of very low level of energy that has not been possible to harness, due to its very low amplitude, very low frequency, or both. Using a CNT sheet flutter device, minor air movements (see Supplementary Information 4) and even ordinary conversation can be transformed into electricity using EMI.

Generation of electricity from everyday conversation perhaps best illustrates the ability of CNT sheet to capture extremely low energy levels. The conversation generates a sound wave which causes the CNT sheet to vibrate, and this vibration produces electricity through EMI. When acoustic wave, a longitudinal wave, propagates through the nanotube sheet, air molecules oscillate in the direction of the wave propagation, which results in compressions and rarefactions of air molecules in the nanotube sheet aerogel. The pressure of air molecules is large enough to produce oscillation of the nanotube strings of the sheet. The nanotube sheet flutter employs electromagnetic induction arising from the motion of nanotube sheet in magnetic field. Therefore, the flapping motions of the nanotubes induced by acoustic wave generate alternating electromotive force in the sheet.

For the demonstration, a sound pressure level of 53 dB (relative to a reference pressure of 20 μPa) was chosen, which is intermediate between quiet office (~50 dB) and ordinary conversation (~60 dB)[26]. As one might expect, the highest voltage would be produced when the acoustic frequency coincides with the resonance frequency of the CNT sheet in the EM induction device. Figure 3a shows the voltage produced by the device (V_{rms}, root mean square voltage) as a function of acoustic frequency. It can be seen that the maximum output voltage (55 μV) is realized at the resonance frequency of 45 Hz. Significant voltage outputs can be obtained at harmonic resonance frequencies, *i.e.*, 90, 135, and 180 Hz, but the voltage output decreases as the resonance frequency increases, since the oscillation amplitude of the CNT sheet at a higher-order resonance mode is smaller than that for a lower-order mode[27]. Alternating output voltages at the resonance frequencies are shown in the inset of Figure 3a. The voltage generation of the flutter device is continuous and stable, as shown in Supplementary Figure S4, for measurements over a 10 hour period.

To assess the extent to which the CNT sheet can capture low energy, the sound pressure level was decreased from 53 dB to 29 dB (equivalent to the sound level of a whisper) in successive experiments at the resonance frequency of 45 Hz, and the results are shown in Figure 3b. As shown in the inset of the figure, even a whisper can be captured by the CNT sheet flutter device and utilized to deliver a voltage of 4 μV. The output power derived from the acoustic energy was also evaluated from the square of root-mean-square voltage divided by the resistance of the sheet ($P=V_{rms}^2/R$). Maximum power output can be delivered to an electrical load when its resistance is equal to the resistance of the nanotube sheet flutter (~9.7 kohm). The maximum specific power (normalized to the sheet weight and area) of ~26 μW/g·m^2 was obtained from an acoustic pressure level of 53 dB, as shown in Figure 3b. The output power exponentially increases with increasing sound pressure level. This result is quite reasonable because sound pressure level is a logarithmic measure of the effective sound pressure relative to a reference value[28].

Infrasound detection. The above described first order acoustic resonance at 45 Hz for the CNT-sheet EMI device resulted from using a CNT sheet that is 5.5 cm long between the electrodes. The fact that the resonance frequency is quite low, and that the resonance frequency is inversely proportional to the sheet length, prompted us to look into the possibility of detecting infrasound by frequency resonance of a CNT sheet. Infrasound is sound that is lower in frequency than 20 Hz, which is inaudible to human ears.

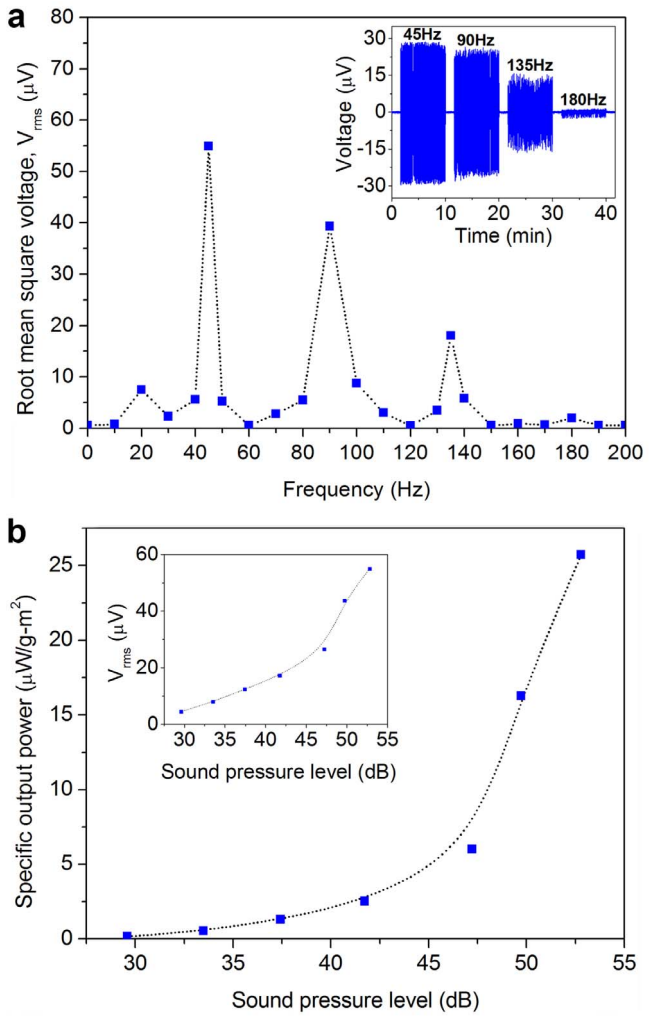

Figure 3 | Generation of electricity from the sound pressure level of ordinary conversation. (a) The dependence of generated voltage on acoustic frequency. A sound pressure level of 53 dB was applied to the flutter. Alternating output voltages at the resonance frequencies are shown in the inset. (b) The specific output power generated at various sound pressure levels at the resonance frequency of 45 Hz. The inset shows the dependency of V_{rms} on the sound pressure level.

Propagation of infrasound precedes natural disasters such as earthquake and volcanic eruption. Therefore, detection of infrasound is utilized for monitoring natural disaster threats[29–32], as well as man-made events, such as rocket launchings[33–36]. While other infrasound detection apparatus are available[37,38], a much simpler and less costly detector would be highly desirable.

To demonstrate the feasibility of utilizing the simple, inexpensive electromagnetic induction device for detecting infrasound, a 12 cm long CNT sheet was utilized. Figure 4 shows the normalized oscillation amplitude that results under ambient conditions when the driving frequency is varied from 1 to 19 Hz when using an applied AC peak-to-peak voltage of 10 V. A first order sheet resonance at 14 Hz is indicated, which indicates that infrasound propagating at this frequency can be detected by the EMI device, by inducing resonant vibration of the sheet, which provides electrical voltage signals (as in the inset of Figure 3a) for detection. It is, therefore, possible that an array of CNT sheets with different sheet lengths could be deployed to detect a range of frequency of infrasound below 20 Hz. It should be noted in this regard that the simple CNT sheet device can detect relatively quiet infrasound below 30 dB.

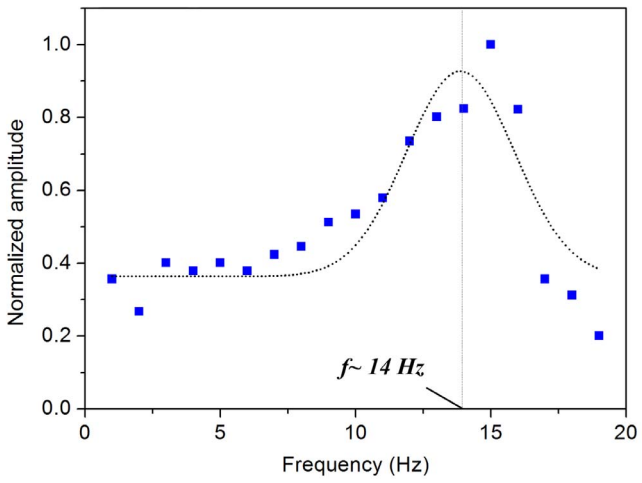

Figure 4 | The frequency dependence of normalized oscillation amplitude when the driving frequency was varied from 1 to 19 Hz using an AC voltage of 10 V (under ambient conditions). The detected resonance for the CNT sheet is at 14 Hz.

Discussion

The carbon nanotube aerogel sheets have unique characteristics that enable the EMI flutter devices. Together with usefully high electronic conductivities, these include air-like densities and MWNT length/diameters ratios that can exceed 40,000, which provide an extremely low force constant for elastic bending. We have exploited these characteristics in simple, inexpensive EMI flutter devices to provide actuation at mV voltages, energy harvesting from mild air perturbations, and to suggest likely applicability for infrasound detection.

Methods

Deposition of Al films onto CNT sheet. The MWNTs and MWNT bundles in MWNT sheets were coated with Al by thermal evaporation deposition. The deposition rate and thickness were monitored using a quartz crystal microbalance (QCM). A MWNT sheet suspended between a pair of copper wire electrodes was attached to a sample holder in such a way that the sheet plane was perpendicular to the evaporation incident angle. During evaporation the substrate was rotated to obtain a uniformly coated sheet. The deposition rate was 1.0 nm/s for all depositions and the vacuum was maintained below 10^{-6} Torr.

Instruments and measurements. The sound pressure level was measured at a distance 5 cm away from a speaker by a sound level meter (B&K Type 4189 microphone) with a detection diameter of 12.7 mm. The same experimental setup was used for acoustic energy harvesting experiments using a nanotube sheet flutter. The data acquisition equipment was LMS SCADAS3 (LMS). All acoustic measurements were performed in a semi-anechoic room. The resistance of the nanotube sheet suspended between a pair of copper wire electrodes was measured using a voltage–current meter (Keithley 2000 multimeter). Scanning electron microscopy (SEM) images were obtained a Hitachi S-4800 field-emission microscope by using an acceleration voltage of 10–15 KeV.

1. Cheng, D. K. *Field and wave electromagnetics.* (Addison-Wesley, New York, 1989).
2. Wu, Y. *et al.* Determination of the young's modulus of structurally defined carbon nanotubes. *Nano Lett.* **8**, 4158–4161 (2008).
3. Dagher, M., Chamanara, N., Sounas, D., Martel, R. & Caloz, C. Theoretical investigation of traveling-wave amplification in metallic carbon nanotubes biased by a DC field. *IEEE Trans. Nanotechnol.* **11**, 463–471 (2012).
4. Jensen, K., Girit, C., Mickelson, W. & Zettl, A. Tunable nanoresonators constructed from telescoping nanotubes. *Phys. Rev. Lett.* **96**, 215503 (2006).
5. Zhang, M. *et al.* Strong, transparent, multifunctional, carbon nanotube sheets. *Science* **309**, 1215–1219 (2005).
6. Edwards, D. L. *et al.* Electron Radiation Effects on Candidate Solar Sail Material. *High Perform. Polym.* **16**, 277–288 (2004).
7. Aliev, A. E. *et al.* Giant-stroke, superelastic carbon nanotube aerogel muscles. *Science* **323**, 1575–1578 (2009).
8. Sapmaz, S., Blanter, Y. M., Gurevich, L. & Van der Zant, H. Carbon nanotubes as nanoelectromechanical systems. *Phys. Rev. B* **67**, 235414 (2003).
9. Tooley, M. *Electronic Circuits: Fundamentals and Applications.* (Elsevier, 2006).

10. Bhiladvala, R. B. & Wang, Z. J. Effect of fluids on the Q factor and resonance frequency of oscillating micrometer and nanometer scale beams. *Phys. Rev. E* **69**, 036307 (2004).
11. Chen, C. *et al.* Nanoscale fluid-structure interaction: Flow resistance and energy transfer between water and carbon nanotubes. *Phys. Rev. E* **84**, 046314 (2011).
12. Chen, C., Ma, M., Zhe Liu, J., Zheng, Q. & Xu, Z. Viscous damping of nanobeam resonators: Humidity, thermal noise, and a paddling effect. *J. Appl. Phys.* **110**, 034320 (2011).
13. Chen, L. *et al.* High-Performance, Low-Voltage, and Easy-Operable Bending Actuator Based on Aligned Carbon Nanotube/Polymer Composites. *ACS Nano* **5**, 1588–1593 (2011).
14. Kim, O., Shin, T. J. & Park, M. J. Fast low-voltage electroactive actuators using nanostructured polymer electrolytes. *Nat. Commun.* **4** (2013).
15. Mitcheson, P. D., Yeatman, E. M., Rao, G. K., Holmes, A. S. & Green, T. C. Energy harvesting from human and machine motion for wireless electronic devices. *Proc. IEEE* **96**, 1457–1486 (2008).
16. Paradiso, J. A. & Starner, T. Energy scavenging for mobile and wireless electronics. *Pervasive Comput.* **4**, 18–27 (2005).
17. Que, R. *et al.* Flexible Nanogenerators Based on Graphene Oxide Films for Acoustic Energy Harvesting. *Angew. Chem. Int. Ed.* **124**, 5514–5518 (2012).
18. Yang, J. *et al.* Triboelectrification-Based Organic Film Nanogenerator for Acoustic Energy Harvesting and Self-Powered Active Acoustic Sensing. *ACS Nano* **8**, 2649–2657 (2014).
19. Wu, L.-Y., Chen, L.-W. & Liu, C.-M. Acoustic energy harvesting using resonant cavity of a sonic crystal. *Appl. Phys. Lett.* **95**, 013506 (2009).
20. Aichao, Y. *et al.* Enhanced Acoustic Energy Harvesting Using Coupled Resonance Structure of Sonic Crystal and Helmholtz Resonator. *Appl. Phys. Express* **6**, 127101 (2013).
21. Cha, S. N. *et al.* Sound-Driven Piezoelectric Nanowire-Based Nanogenerators. *Adv. Mater.* **22**, 4726–4730 (2010).
22. Guo, H. *et al.* A nanogenerator for harvesting airflow energy and light energy. *J. Mater. Chem. A* **2**, 2079–2087 (2014).
23. Sun, C., Shi, J., Bayerl, D. J. & Wang, X. PVDF microbelts for harvesting energy from respiration. *Energy Environ. Sci.* **4**, 4508–4512 (2011).
24. Lee, S. *et al.* Super-Flexible Nanogenerator for Energy Harvesting from Gentle Wind and as an Active Deformation Sensor. *Adv. Funct. Mater.* **23**, 2445–2449 (2013).
25. Lee, J.-H. *et al.* Highly sensitive stretchable transparent piezoelectric nanogenerators. *Energy Environ. Sci.* **6**, 169–175 (2013).
26. Raphael, L. J., Borden, G. J. & Harris, K. S. *Speech Science Primer: Physiology, Acoustics, and Perception of Speech.* (Lippincott Williams & Wilkins, 2007).
27. Craig, R. R. *Structural dynamics: an introduction to computer methods.* (Wiley, New York, 1981).
28. Ingard, U. *Acoustics.* (Jones & Bartlett Learning, 2008).
29. Ulivieri, G. *et al.* Monitoring snow avalanches in Northwestern Italian Alps using an infrasound array. *Cold Reg. Sci. Technol.* **69**, 177–183 (2011).
30. Dabrowa, A. L., Green, D. N., Rust, A. C. & Phillips, J. C. A global study of volcanic infrasound characteristics and the potential for long-range monitoring. *Earth Planet. Sci. Lett.* **310**, 369–379 (2011).
31. Johnson, J. B. & Ripepe, M. Volcano infrasound: A review. *J. Volcanol. Geoth. Res.* **206**, 61–69 (2011).
32. Walker, K. T. *et al.* An analysis of ground shaking and transmission loss from infrasound generated by the 2011 Tohoku earthquake. *J. Geophys. Res. -Atmos.* **118**, 12,831–12, 851 (2013).
33. Der, Z. A., Shumway, R. H. & Herrin, E. T. *Monitoring the Comprehensive Nuclear-Test-Bant Treaty: Data Processing and Infrasound.* (Birkhäuser Basel, 2002).
34. Hedlin, M. A. H., Walker, K., Drob, D. P. & de Groot-Hedlin, C. D. Infrasound: Connecting the Solid Earth, Oceans, and Atmosphere. *Annu. Rev. Earth Planet. Sci.* **40**, 327–354 (2012).
35. Le Pichon, A., Garcés, M., Blanc, E., Barthélémy, M. & Drob, D. P. Acoustic propagation and atmosphere characteristics derived from infrasonic waves generated by the Concorde. *J. Acoust. Soc. Am.* **111**, 629–641 (2002).
36. Bass, H. E. *et al.* Infrasound. *Acou. Today* **2**, 9–19 (2006).
37. Alcoverro, B. & Le Pichon, A. Design and optimization of a noise reduction system for infrasonic measurements using elements with low acoustic impedance. *J. Acoust. Soc. Am.* **117**, 1717–1727 (2005).
38. Zumberge, M. A. *et al.* An optical fiber infrasound sensor: A new lower limit on atmospheric pressure noise between 1 and 10 Hz. *J. Acoust. Soc. Am.* **113**, 2474 (2003).

Acknowledgments

This research was supported by the National Research Foundation of Korea (Grants 2009-0083512, 2011-0024818, 2014R1A2A1A05007760, and 2014R1A1A4A01008768), Defense Acquisition Program Administration and Agency for Defense Development under Contract UD100048JD, Pusan National University Research Grant 2012, the Civil & Military Technology Cooperation Program through the National Research Foundation of Korea (NRF) funded by the Ministry of Science, ICT & Future Planning (No. 2013M3C1A9055407), Air Force Office of Scientific Research grant FA9550-12-1-0211, and Robert A. Welch Foundation Grant AT-0029. The authors also acknowledge support from the Institute of Advanced Aerospace Technology at Seoul National University.

Author contributions

T.J.K. contributed to this work in experiment planning, experiment measurements, data analysis and manuscript preparation. T.K. contributed to experiment measurements and data analysis, E.Y.J. and H.I. prepared the samples and performed experimental measurements. The nanotube samples were prepared and characterized by X.L.-C., R.O.-R., J.O. and M.E.K. R.H.B., H.H.L. and Y.H.K. contributed to experiment planning, data analysis and manuscript preparation.

Additional information

Supplementary information accompanies this paper at http://www.nature.com/scientificreports

Competing financial interests: The authors declare no competing financial interests.

How to cite this article: Kang, T.J. *et al.* Nanotube Aerogel Sheet Flutter for Actuation, Power Generation, and Infrasound Detection. *Sci. Rep.* **4**, 6105; DOI:10.1038/srep06105 (2014).